Biomedical Signal Processing and Control 97 (2024) 106719

Contents lists available at ScienceDirect

Biomedical Signal Processing and Control

journal homepage: www.elsevier.com/locate/bspc

Beta-band cortico-muscular phase coherence in hemiparetic stroke

Nishaal Parmar [a,1], Parikshat Sirpal [a,1], William A Sikora [b], Julius P.A. Dewald [c,d], Hazem H. Refai [a], Yuan Yang [c,e,f,g,*]

[a] University of Oklahoma, School of Electrical and Computer Engineering, Gallogly College of Engineering, Norman, OK, United States of America
[b] University of Oklahoma, Stephenson School of Biomedical Engineering, Norman, OK, United States of America
[c] Northwestern University, Department of Physical Therapy and Human Movement Sciences, Chicago, IL, United States of America
[d] Northwestern University, Department of Biomedical Engineering, Evanston, IL, United States of America
[e] University of Illinois Urbana-Champaign, Department of Bioengineering, Grainger College of Engineering, Urbana, IL, United States of America
[f] Carle Foundation Hospital, Stephenson Family Clinical Research Institute, Clinical Imaging Research Center, Urbana, IL, United States of America
[g] University of Illinois Urbana-Champaign, Beckman Institute for Advanced Science and Technology, Urbana, IL, United States of America

ARTICLE INFO

Keywords:
Multimodal corticomuscular connectivity
Phase coherence analysis
Post-stroke neuroadaptation
Electroencephalography
Electromyography
Beta-band phase coherence

ABSTRACT

Following a stroke, compensation for the loss of ipsilesional corticospinal and corticobulbar projections, results in increased reliance on contralesional motor pathways during paretic arm movement. Better understanding outcomes of post-stroke contralesional cortical adaptation outcomes may benefit more targeted post-stroke motor rehabilitation interventions. This proof-of-concept study involves eight healthy controls and ten post-stroke participants. Electroencephalographic (EEG) and deltoid electromyographic (EMG) data were collected during an upper-limb task. Phase coupling between beta-band motor cortex EEG and deltoid EMG was assessed using the Multi-Phase Locking Value (M−PLV) method. Different from classic cortico-muscular coherence, M−PLV allows for the calculation of dynamic phase coherence and delays, and is not affected by the non-stationary nature of EEG/EMG signals. Nerve conduction delay from the contralateral motor cortex to the deltoid muscle of the paretic arm was estimated. Our results show the ipsilateral (contralesional) motor cortex beta-band phase coherence behavior is altered in stroke participants, with significant differences in ipsilateral EEG-EMG coherence values, ipsilateral time course percentage above the significance threshold, and ipsilateral time course area above the significance threshold. M−PLV phase coherence analysis provides evidence for post-stroke contralesional motor adaptation, highlighting its increased role in the paretic shoulder abduction task. Nerve conduction delay between the motor cortices and deltoid muscle is significantly higher in stroke participants. Beta-band M−PLV phase coherence analysis shows greater phase-coherence distribution convergence between the ipsilateral (contralesional) and contralateral (ipsilesional) motor cortices in stroke participants, which is interpretable as evidence of maladaptive neural adaptation resulting from a greater reliance on the contralesional motor cortices.

1. Introduction

Stroke is the third leading cause of long-term adult disability in the United States [61], affecting nearly 800,000 Americans each year and is expected that the incidence of stroke will rise by approximately 80 % by 2038 [43]. Approximately 80 % of stroke survivors over 65 years old show reduced post-stroke mobility of the paretic arm, [61], frequently expressed as a loss of independent joint control resulting in limb synergies [6,52,44,32,37]. Following a hemiparetic stroke, performing a shoulder abduction effort with the paretic arm frequently results in a coupled response in wrist and finger flexors, known as flexion synergy, leading to an inability to completely open the hand, as well as a decrease in grasping force control [32,38]. Likewise, a reaching motion of the paretic arm often causes abnormal muscle coactivation between the shoulder abductors and elbow flexors, leading to decreased independent control of joint movement resulting in a reduction in the shoulder and elbow range of motion, and an overall decrease in the total reaching work area covered by the paretic limb [52]. The residual disabilities

* Corresponding author at: University of Illinois Urbana-Champaign, Department of Bioengineering, Grainger College of Engineering, Urbana, IL, United States of America (Y. Yang).
E-mail address: yuany@illinois.edu (Y. Yang).
[1] Equally contributing authors.

https://doi.org/10.1016/j.bspc.2024.106719
Received 10 February 2024; Received in revised form 26 June 2024; Accepted 1 August 2024

associated with the loss of independent joint control in the paretic upper limb result in difficulty performing basic daily activities, leading to a decrease in quality of life [53]. Over 50 % of stroke survivors continue to suffer from paretic upper limb motor impairments for months to years after a stroke [36], generally experiencing a lower health-related quality of life a year after the incident [22,69]. The primary method of post-stroke care concentrates on intervention via upper limb neuro-rehabilitation [31], using movement-limited task-specific repetitive limb training, potentially with robotic assistance [60,21]. Due to the ongoing nature of post-stroke disability, sustained intensive rehabilitation therapy programs may offer additional improvement in limb functionality even in the chronic (>6 months) stage of the disease, yet many stroke survivors are only offered a single short-term therapy program [54], with 55–85 % of potential recovery often being assumed to occur within 3–6 months post-stroke in a majority of the population [58].

More recently, advances in stroke rehabilitation therapy have introduced electrostimulation therapy of the upper limb [75], invasive deep brain neurostimulation [2], non-invasive neurostimulation techniques such as transcranial direct current stimulation [35] and transcranial magnetic stimulation [1], and robot-assisted therapy [15]. Robotic therapy allows for independent, unsupervised patient rehabilitation exercises that can deliver customized task-driven training to patients [16]. Robotic therapy has been shown to provide comparable outcomes to more traditional task-oriented occupational therapy or physiotherapy in poststroke rehabilitation [8], although it has not been shown to be a cost-effective solution compared to a similar level of traditional therapy [49]. A hybridized approach consisting of both robotic therapy and Functional Electrical Stimulation of the affected limb may prove more effective [28]. Any optimization in post-stroke recovery outcomes remains a priority in patient care, as current rehabilitation treatments are minimally effective in the recovery of upper-limb functionality in moderate-to-severely impaired individuals [39,48]. An exception is the use of progressive shoulder abduction loading, using impairment-based robotics [12], which has shown promise in increasing reaching function in this cohort [13,15,16].

Previous post-stroke neuroimaging studies have demonstrated that during the post-stroke rehabilitation process, neural adaptation of muscle control of the paretic arm often involves increased neural activity in the contralesional motor areas which are ipsilateral to the paretic side [24]. This increased motor-cortex neuroplasticity is not limited to the post-stroke recovery process, but is known to be a standard response to traumatic brain injury, although the exact mechanism of neurogenesis remains unknown (YouRong et al, 2015). This response is present in individuals with moderate to severe chronic stroke, suggesting that contralesional sensorimotor cortex reorganization is a common post-stroke neural adaptation and is associated with impairment severity [18,19,65]. In contrast, healthy individuals primarily show activity in the motor cortex contralateral to arm movement. In individuals with hemiparetic stroke, abnormal flexion synergy [52,32,37,38] and increased spasticity [34,72,14] is routinely observed in the paretic upper limb. This abnormal co-activation of paretic arm shoulder abductor and elbow flexor muscles is likely due to the increased reliance on ipsilateral cortico-reticulospinal pathways in post-stroke upper limb movement of the affected arm [37]. Recent diffusion tensor imaging (DTI) studies have shown that structural changes in contralesional indirect cortico-reticulospinal motor pathways post-stroke are linked to the level of motor impairment [5,29,44]. The implication of these structural findings, as well as high-density EEG findings [37], is that an increased use of the contralesional cortico-reticulospinal pathway is linked to motor impairment such as the expression of the upper extremity flexion synergy, resulting in a reduction of reaching and hand opening abilities post-stroke and, thus, being related to suboptimal motor recovery outcomes. Therefore, determining the ipsilesional and contralesional cortico-muscular time delay changes post stroke can be indicative of damage to the corticospinal tract (CST−ispilesional), as well as the signal transmission in the contralesional cortico-reticulospinal pathway [51,55].

Scalp EEG, a widely accepted technique for monitoring human brain activity [50], was used to measure beta-band (15–25 Hz) ipsilesional and contralesional motor cortex activity, as beta band activities recorded at the sensorimotor areas have been shown to play a functional role in the execution of human object-directed actions [41]. Beta-band activities have been shown to be correlated to the electrical activity of the upper-limb deltoid muscle during an abduction task, recorded via electromyography (EMG)[55]. EEG-EMG connectivity is a common method used for the quantization of sensorimotor connectivity, and is indicative of both direct and indirect cortico-spinal interactions [55].

EEG-EMG connectivity analysis is typically calculated using the coherence method, i.e., cortico-muscular coherence (CMC). CMC may be used to detect and quantify the motor coupling between limb musculature and the motor cortex, providing a versatile yet non-invasive tool for the analysis of human motor tasks. In recent studies, CMC has been used to understand and quantify the effects of upper and lower limb movements in both normal movement control and stroke rehabilitation. The beta-band upper-limb CMC is a critical indicator of motor cortical and muscular coupling during hand movement tasks [77]. Further analysis of upper-limb CMC during the reach-to-grasp task shows that CMC is altered by changing the amount of weight lifted during the task [25]. In lower-limb studies, CMC is often used to analyze stance, walking gait, and stability, with the change of CMC associated with gait pattern [10], age[10,71]and balance [62]. In stroke survivors, brain-controlled muscle movement and corticomuscular control are significantly altered [30], with CMC changing during the post-stroke recovery period [64]. The reduction of ipsilesional CMC is a key indicator of the impairment of brain-controlled muscle movement [23]. During the post-stroke recovery period, increased CMC values are indicative of greater functional movement ability of both the lower and upper limbs [30,70]. CMC has also been used in post-stroke closed-loop motor rehabilitation for both machine-assisted therapy [76]and brain-computer-interface based intervention [9,47,30]. The utilization of CMC may help enhance the accuracy of EEG-based BCI systems [25,77]. However, previous CMC work did not account for the non-stationary nature of EEG-EMG signals that occur during movement.

In contrast to the CMC research discussed above, EEG-EMG connectivity in the current study was analyzed via a phase coherence measure [59]. We investigated both ipsi- and contra-lesional brain activities and their coupled muscle activities in stroke brains via a newly developed the Multi-Phase Locking Value (M−PLV) method [59]. M−PLV allows for the calculation of dynamic phase coherence and delays, not biased by non-stationary nature of EEG/EMG signal. This is different from the classic CMC which is influenced by both phase and amplitude dynamics [3]. We show changes in the cortico-spinal connectivity of stroke participants in comparison to healthy controls. A better understanding of the mechanisms involved in this process may enhance future assessments of motor recovery using the proposed method, improving stroke upper-limb motor recovery outcomes and providing insight into the extent of post-stroke contralesional neurological reorganization.

2. Materials and methods

2.1. Data collection

All data collected in this study was approved by the Institutional Review Board (IRB) at Northwestern University (STU0021840), and participants provided informed consent prior to study participation [55]. All participants have signed a consent form allowing their photographs to be used in publications. Data was collected from eight healthy control participants with no history of stroke or seizure and ten chronic hemiparetic participants with stroke-related neurological damage confined to a single hemisphere and varying degrees of post-stroke

paretic arm motor impairment, (as measured by the Fugl-Meyer post-stroke motor assessment test), at least a year post-stroke [Table 1].

Each participant was seated securely in a Biodex System 3 Pro testing and rehabilitation device, consisting of an adjustable chair, track, and attached Biodex pedestal, and strapped in via shoulder and lap restraints. This Biodex system was used to position the participant, as well as collect post-stroke physical impairment data, such as arm position, velocity, and torque measurements. In order to collect additional impairment data, a custom robotic device [57] was connected to the Biodex system. This device consisted of a forearm weight-support platform, and a 6-DOF load cell (JR3, Woodland, CA) which was able to measure participants' shoulder abduction (SABD) and elbow flexion (EF) torques. Each participant's forearm was rigidly attached to the Biodex/device assembly using a fiberglass forearm-wrist-hand cast, which was inserted with a Delrim cuff into a metal ring. As shown in [Fig. 1], the participant's upper limb was positioned with 85° shoulder abduction, 45° shoulder flexion, 0° shoulder rotation, and 90° elbow flexion, with the medial epicondyle of the humerus aligned with the center of rotation of the actuator. In participants with a hemiparetic stroke, the paretic arm was selected for study. For control participants, a random arm was selected, and all trials were conducted using that arm.

Prior to data collection, the maximum voluntary torque (MVT) for shoulder abduction (SABD) was recorded in each study participant by requesting them to maximally 'lift up' their arm for 5 s. All stroke participants were able to generate a measurable EMG response in the deltoid muscle of the paretic limb during this test. These data were filtered with a moving median filter (250 ms window, with a 1 ms step) online. This movement was repeated until 3 consecutive trials were recorded with peak variance within 5 % of each other, with the peak average of the final three trials as the recorded MVT value. Each participant was then asked to perform 25 movement task trials, during which data was collected from a 32-channel EEG cap (Biosemi, Inc, Active II, Amsterdam, the Netherlands) and 2 Biosemi EMG electrodes placed 1 cm apart on the intermediate deltoid muscle. Data was sampled at 2048 Hz, with all electrode impedances kept under 25 kΩ. For each task trial, the study participant was given an auditory cue and asked to abduct the tested arm at the shoulder to 20 % of the measured MVT value, then generate that torque for 10 s once the 20 % MVT value was reached. To minimize the onset of inter-trial fatigue, participants were asked to relax their arm fully for at least 1 min between trials. Additionally, visual feedback was provided to the participant to indicate deviation from the desired MVT abduction percentage. If a trial's SABD torque measured over 10 % error off the target torque, the trial was discarded, and the participant was asked to pause, relax, and restart the trial after enough rest.

Table 1
Demographic information of the eight healthy and ten stroke participants. Post-stroke paretic arm motor control for stroke participants was measured by the Fugl-Meyer motor assessment test (FMA), with a maximum Upper Extremity Fugl-Meyer score of 66. Lower scores indicate individuals with an increased level of upper limb motor impairment.

Participant Number	Gender	Age	Dominant Hand	Affected/ Tested Arm	FMA Score	Years Since Stroke
Control 1	M	64	R	R	–	–
Control 2	M	75	L	R	–	–
Control 3	M	55	R	L	–	–
Control 4	F	55	R	L	–	–
Control 5	F	64	R	R	–	–
Control 6	M	60	R	R	–	–
Control 7	M	60	R	R	–	–
Control 8	F	73	R	L	–	–
Stroke 1	M	49	L	L	30	9
Stroke 2	M	59	L	L	19	11
Stroke 3	M	60	L	R	26	4
Stroke 4	M	72	R	L	49	8
Stroke 5	M	74	R	L	13	16
Stroke 6	M	65	R	L	22	8
Stroke 7	M	65	R	L	49	4
Stroke 8	F	67	R	R	24	1.5
Stroke 9	F	71	R	R	8	16
Stroke 10	M	62	R	L	40	5

Fig. 1. Experimental subject positioning for the shoulder movement task, with subject seated in the Biodex 3 chair, with arm securely fastened to the Biodex pedestal via a custom cast with Delrim cuff, weight-support platform, and load cell.

2.2. Multimodal EEG-EMG data preprocessing

Multimodal EEG-EMG trial data was extracted from each participant. EEG data was collected from the EEG electrodes above the left and right motor cortices (C3 and C4), while EMG data was collected from a pair of deltoid EMG electrodes. The two EMG electrode values were subtracted from each other to calculate a single EMG channel. The EEG data was re-referenced to average via EEGLAB [11], and then both the EEG and EMG data were notch-filtered at 60 Hz to remove electrical noise. The DC component was removed from the deltoid EMG channel, and rectified, in order to increase the expression of low-frequency action potentials [20,42]. Finally, all EEG and EMG channels were band-pass filtered at the desired frequency range (15–25 Hz, corresponding to the center of the beta EEG signal band). The beta band was chosen as beta band activities recorded at the sensorimotor areas have been shown to play a functional role in the execution of human task-directed motor actions [41]. For each of the 25 trials, any trials containing artifacts or incomplete data were removed, and trial data was segmented into non-overlapping epochs of 1 s in length, giving a maximum of 250 epochs per participant, similar to the windowing procedure used for CMC calculation in [7]. Neuromuscular delay and phase coherence between the deltoid EMG signals and the ipsilateral (contralesional) and contralateral (ipsilesional) EEG signals were calculated using multi-phase locking value (M−PLV), which, given two data time series, generates a value between 0 and 1, with 1 indicating the two timeseries are perfectly phase-coherent, and 0 indicating no phase coupling between the two data sets [59].

2.3. Multi-Phase Locking value data analysis

Multi-Phase Locking Value (M−PLV) [59] was utilized to determine the cortio-muscular interactions for both contralateral (ispilesional for stroke) and ipsilateral (contralesional) motor pathways and their time delays, using EEG as the input signal and EMG as the output signal.

M−PLV allows for the quantization of phase coupling between two time series signals. M−PLV is derived from the earlier techniques of Multi-Spectral Phase Coherence (MSPC) [27] and Phase Locking Value (PLV) [17], and can be used to quantize *m*:*n* phase locking and phase delay across multiple non-integer resonant frequencies. The quantized phase coupling between two signals, M−PLV (ψ), is be calculated as [55,59]

$$\psi(f_1, f_2 \cdots f_n; m_1, m_2 \cdots m_n; t; \tau) = \left| \frac{1}{K} \sum_{k=1}^{K} exp\left(j\left(\sum_{l=1}^{L} (m_l \phi_k(f_l, t-\tau)) - n\phi_k(f_\Sigma, t) \right) \right) \right| \quad (1)$$

where K is the number of observations (epochs/trials), m_l and n are the input and output coupling frequencies under calculation, and τ is the output delay value. $\phi_k(f_l, t)$ and $\phi_k(f_\Sigma, t)$ represent the instantaneous phase at the k^{th} observation of the input (f_l) and output (f_Σ) data. This instantaneous phase, in the form of a narrowband filtered timeseries with a spectrum centered on the coupling frequencies, may be directly obtained from the Hilbert transform [4].

In the present study, the frequency relationship *m*:*n* is 1:1, and$f_l = f_\Sigma$, representing the beta-band frequency range of 15–25 Hz. K is the number of epochs under analysis for each participant (maximum 250), and $\phi_i(f_l, t_k)$ and $\phi_o(f_\Sigma, t_k)$ are, respectively, the instantaneous phase values of the bandpass-filtered input and output signals for the K^{th} trial. τ is the calculated response delay latency (nerve conduction delay) between the input EEG (brain) and output EMG (muscle) signals. After these changes, the MPLV equation used in this study represents the phase coherence between the input (ϕ_i) and output(ϕ_o) signals as below:

$$\psi(f_\Sigma; t; \tau) = \left| \frac{1}{K} \sum_{k=1}^{K} exp(j(\phi_i(f_\Sigma, t_k - \tau) - \phi_o(f_\Sigma, t_k))) \right| \quad (2)$$

After determining the response delay latency and appropriately delaying the output EMG signal, M−PLV was used to calculate the coherence value (CV) time courses of the EMG deltoid signal with respect to the ipsilateral and contralateral EEG input signals. For each CV time course, a 95 % M−PLV significance threshold was independently calculated for each input–output dataset pair using a Monte Carlo simulation of the data, a widely accepted measure of statistical significance [63,45].

For each M−PLV time course, in addition to the nerve conduction delay and average CV, the percentage of the duration of each time course above the 95 % significance threshold was recorded, as well as the total area of the time course above the threshold. To calculate the 95 % significance threshold of each CV time course, the Monte Carlo simulation method was used, [59,40,67,68,73]and M−PLV was used to calculate the average CV between the input and the randomized output data after random shuffling of output (i.e., EMG data). This process was repeated 10,000 times, generating a probability distribution of average CV values of the EEG input for that particular time course with respect to the randomized EMG output data. A series of 2-tailed two-sample t-tests were performed, comparing control and stroke participant EMG deltoid data with EEG data both contralateral and ipsilateral to the tested arm (ipsilesional and contralesional, respectively, for stroke participants). For these tests, p values of 95 % ($p \leq 0.05$) indicated statistical significance, showing that the two sampled datasets belong to different population groups with 95 % confidence. For each participant, the phase coherence Laterality Index (LI), which represents a quantitative measure of hemispheric activity dominance [55], was calculated as follows using the average ipsilateral and contralateral coherence values (CV):

$$LI = \frac{contralateralCV - ipsilateralCV}{contralateralCV + ipsilateralCV} \quad (3)$$

3. Results and discussion

3.1. MPLV time course

A sample MPLV CV time course is shown in [Fig. 2]. The dotted red line represents the 95 % significance threshold for this time course data. Other values calculated from each time course include the total time course area above the significance threshold (AAT), the total percentage of time each time course remains above the significant threshold (%AT), the average time course CV value (CV), and the nerve-conduction latency value (τ) between the EEG and EMG signals.

The 10,000 generated CV averages were ordered from lowest to highest, and the 9,500th value was chosen as the 95 % threshold signifying significant phase coherence. The response delay latency for each time course was obtained by delaying the EMG (output) signal through a range of 0–120 ms via increments of 0.488 ms (1/2048 s) and calculating the average coherence value (CV) associated with each input–output signal pair. The delay latency was recorded as the time delay value resulting in the maximum time course-averaged M−PLV CV between the EEG input and EMG delayed-output signals. [Fig. 3] shows an example of this τ calculation for a control participant using a delayed EMG output signal and a contralateral EEG motor cortex input signal, obtaining a delay value τ = 42.97. The M−PLV average CV for this control participant was 0.063, and the average nerve conduction time delay for all control subjects was 29.67 ms, which is a typical nerve conduction time delay value from the brain to the deltoid muscles [46]; Witham et al. 2000).

3.2. Time delay in the corticospinal tract

When comparing the EEG-EMG average CV values contralateral to the tested arm (ipsilesional for stroke participants), control and stroke participant populations are not significantly different [Fig. 4a] (p = 0.24). The CV value ranges calculated fall within expected ranges for beta-band CMC previously reported; [40,66,68,73,74]. However, the effect of the neurological damage present in the ipsilesional hemisphere for stroke participants is observed through the calculated nerve conduction time delay values between the deltoid EMG data for the tested arm and the EEG for the motor cortex contralateral to the tested arm (ipsilesional for stroke participants) [Fig. 4b]. There is a statistically significant difference between control and stroke participants in nerve conduction delays ($p < 0.001$) [Fig. 4b]. Stroke survivors experienced significantly greater nerve conduction delays between the EEG signal from the ipsilesional motor cortex (contralateral to the tested arm) and the EMG signal from the tested muscles (avg. 78.52 ms) when compared with healthy control participants (avg 29.67 ms) [Table 2]. This increased cortico-muscular delay in stroke-affected upper limbs has previously been observed using directed CMC (dCMC) analysis during finger extension motions [78]. One explanation for the increase in nerve conduction delay observed in this study in stroke survivors may be accounted for by the loss of more direct corticospinal projections caused by the stroke.

Despite the observation of a significantly increased contralateral EEG-EMG nerve conduction delay in stroke participants, this study was unable to demonstrate a statistically significant correlation between FMA score in stroke participants and either nerve conduction delay or average CV value. This may be due to the limited study sample size. We theorize that a larger study would be more able to account for individual variation and may observe such a correlation.

3.3. Post-stroke ipsilateral neuroplasticity

In addition to the increased ipsilesional EEG-EMG nerve conduction delay observed in stroke participants, M−PLV analysis also shows neurological changes in the contralesional hemisphere activity of stroke participants. Phase-coherence analysis of post-stroke beta-band EEG-

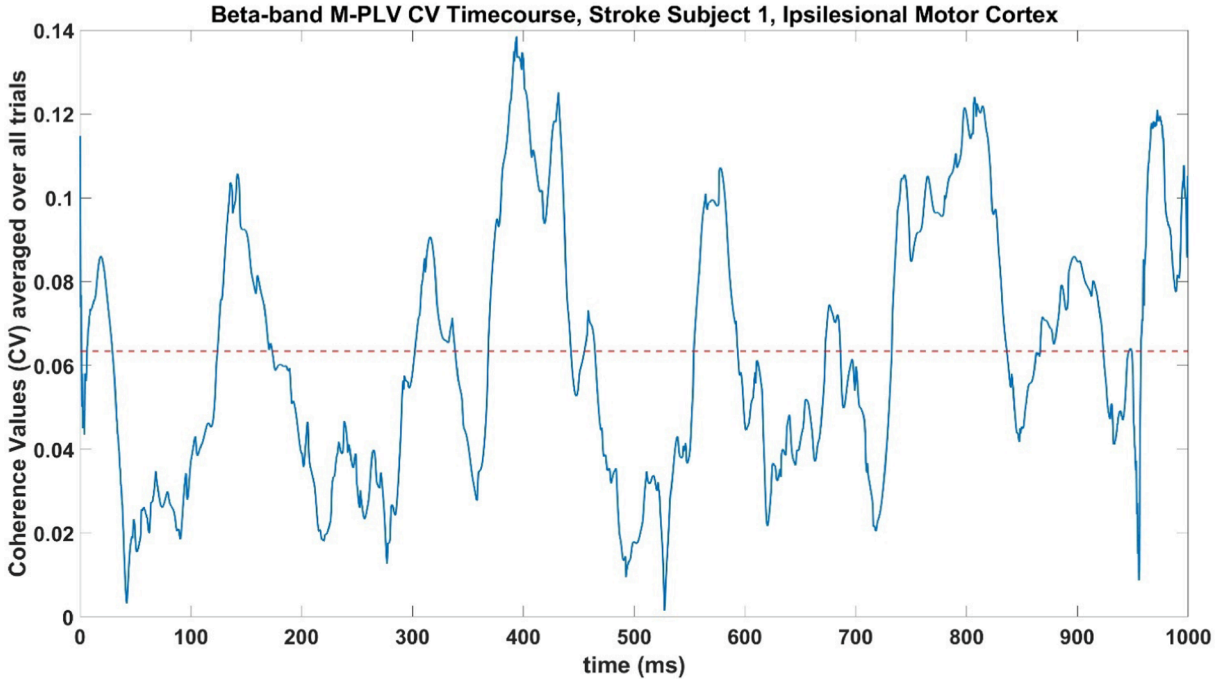

Fig. 2. M−PLV CV time course for a stroke participant, paretic arm EMG vs. contralateral (ipsilesional) motor cortex, $\tau = 89.84$ ms, 95 % significance threshold = 0.0634 (red line), average timecourse CV=0.0666.

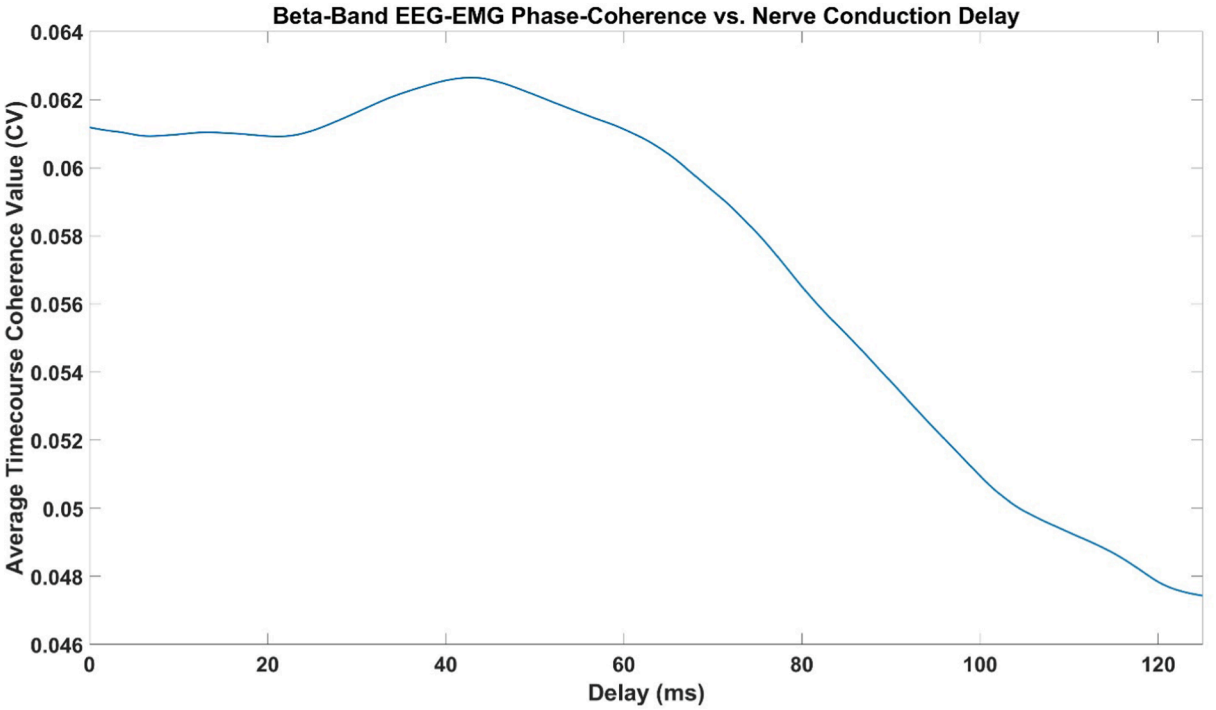

Fig. 3. Optimal delay value (τ) calculation for a control subject, showing an optimal delay value (peak) of 42.97 ms with a 1-second average contralateral beta-band CV of 0.063 across 250 abduction trials.

EMG task data indicates signal convergence between the ipsilateral and contralateral motor cortices during upper-limb movement tasks. This signal convergence provides evidence for post-stroke contralesional neural adaptation. This convergence suggests that the contralesional motor cortex becomes increasingly involved in motor control of the paretic arm during the chronic post-stroke period, and this involvement may be associated with post-stroke motor impairment levels.

Laterality index calculations of the stroke and control participant populations do not result in significant differences at the 95 % or higher confidence levels ($p = 0.27$) [Fig. 5a]. However, when comparing the EMG data with the central EEG ipsilateral motor cortex electrode (contralesional for stroke participants) during shoulder abduction, stroke and control participants are significantly different based on average phase-coherence value, total percentage of lift timecourse

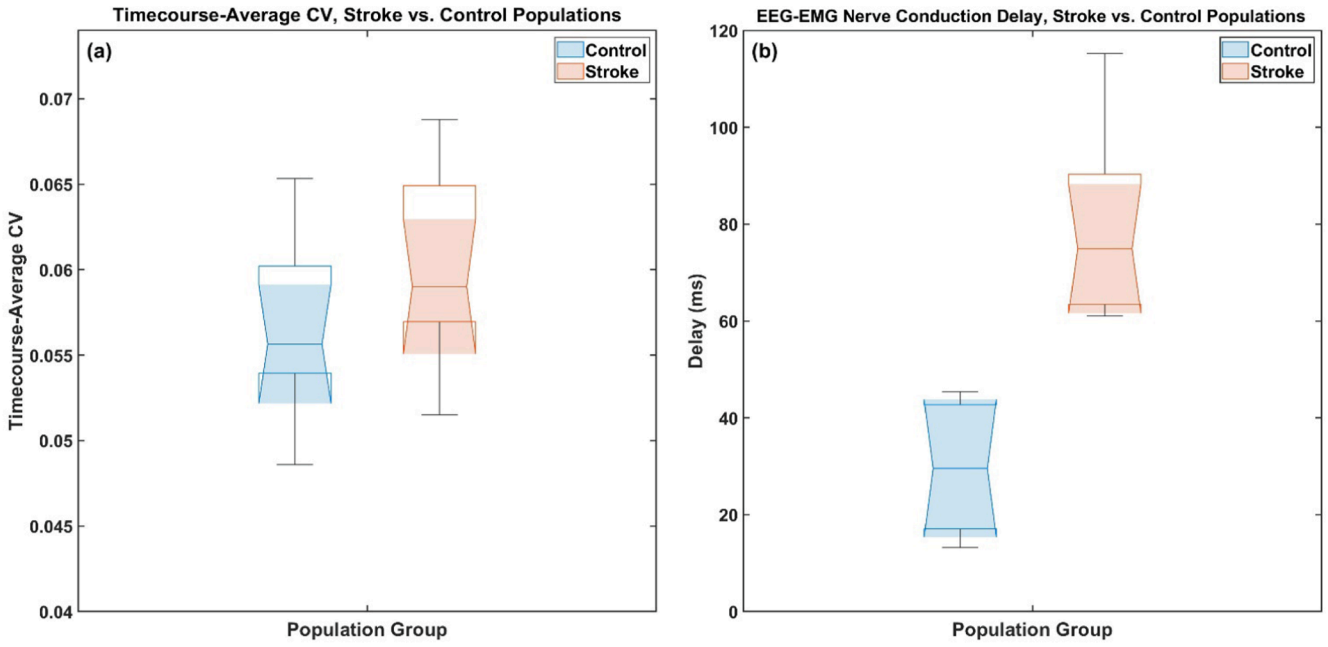

Fig. 4. Fig. 4a (left) showing the EEG-EMG time course-averaged CV data for the tested arm and contralateral motor cortex (ipsilesional for stroke participants). The stroke (red) and control (blue) participants do not represent two statistically different population distributions, with the median CV shown as the line inside the box, and the upper and lower quartiles as box edges, and the range given as the lines above and below the box ($p = 0.24$). Fig. 4b (right) shows the differing nerve conduction time-delay values (left) of control (blue) and stroke (red) participants between the tested arm and contralateral motor cortex (ipsilesional for stroke participants). The stroke and control delay values in Fig. 4b represent two statistically different population distributions, with the median delay shown as the line inside the box, and the upper and lower quartiles as box edges, and the range given as the lines above and below the box ($p < 0.001$, right).

Table 2
Calculated corticomuscular delay values for control and stroke individuals.

Participant Number	Control CorticomuscularDelay (ms)	Stroke CorticomuscularDelay (ms)
1	42.97	89.84
2	20.02	61.04
3	17.08	70.8
4	17.10	64.45
5	42.48	57.49
6	32.74	94.24
7	19.53	59.69
8	45.41	115.23
9		111.33
10		61.04
Mean Delay	29.67	78.52

above the 95 % significance threshold, and graphed area above the significance threshold, all with a high (>95 %) level of likelihood (see Fig. 5b–d). When comparing beta-band average phase-coherence values (CV) between EEG and EMG signals during the abduction task for both stroke and non-stroke participant populations, CV distributions in the motor cortex region ipsilateral to the tested arm are significantly different (i.e. contralesional motor cortex in stroke participants) ($p = 0.032$) [Fig. 5b]. The two populations also exhibit statistically different distributions in the motor cortex when comparing the population time course percentage of each 1-second abduction interval with average CV values above the significance threshold (%AT, $p = 0.0017$) [Fig. 5c] and the total area over this significance threshold (AAT) during the 1-second abduction task in a CV-time plot (AAT, $p = 0.026$) [Fig. 5d]. These distributions indicate that the contralesional motor cortex of chronic stroke survivors (ipsilateral to the paretic/tested arm) behaves significantly differently in the beta-band region during movement tasks when compared to the equivalent motor cortex (ipsilateral to the tested arm) in normal individuals. Individual subject data for ipsilateral average CV, 95 % significance threshold CV, time course percentage above significance threshold, and timecourse area above significance threshold may be found in [Table 3].

We show that the motor cortex ipsilateral to the tested/paretic arm exhibits significantly different beta-band phase coherence behavior between healthy control and chronic stroke participants. Furthermore, for control participants, the ipsilateral and contralateral motor cortices show statistically different behavioral distributions ($p = 0.019$) in the % AT that was over the per-patient CV significance threshold [Fig. 6]. This statistical significance indicates the differing roles of the ipsilateral and contralateral motor cortices in the control of single-limb upper-arm movement tasks. For stroke participantsthe two distributions (stroke ipsilateral and contralateral average CV) converge, however, and are no longer part of two statistically independent populations ($p = 0.66$). Individual subject data for contralateral average CV, 95 % significance threshold CV, timecourse percentage above significance threshold, and timecourse area above significance threshold is shown in Table 4.

Different from previous studies which are mainly focused on the frequency domain analysis [56,26,55], this work unveiled the time-varying dynamic interaction between the brain and muscles during the shoulder abduction task. In this cross-sectional study, the observed post-stroke outcome of phase-coherence distribution convergence is likely related to prior neural adaptation involved following post-stroke recovery [33], though a future longitudinal study during recovery will be needed to justify this assumption. The increased contralesional cortico-muscular interaction may be indicative of use of contralesional cortico-reticulospinal motor pathways given the loss of ipsilesional corticofugal projections when performing the shoulder abduction task [37]. This adaptation may reduce the long-term functional use of the paretic arm due to the expression of flexion synergy, resulting in coactivation of shoulder abductor and elbow, wrist, and finger flexor muscles [44].

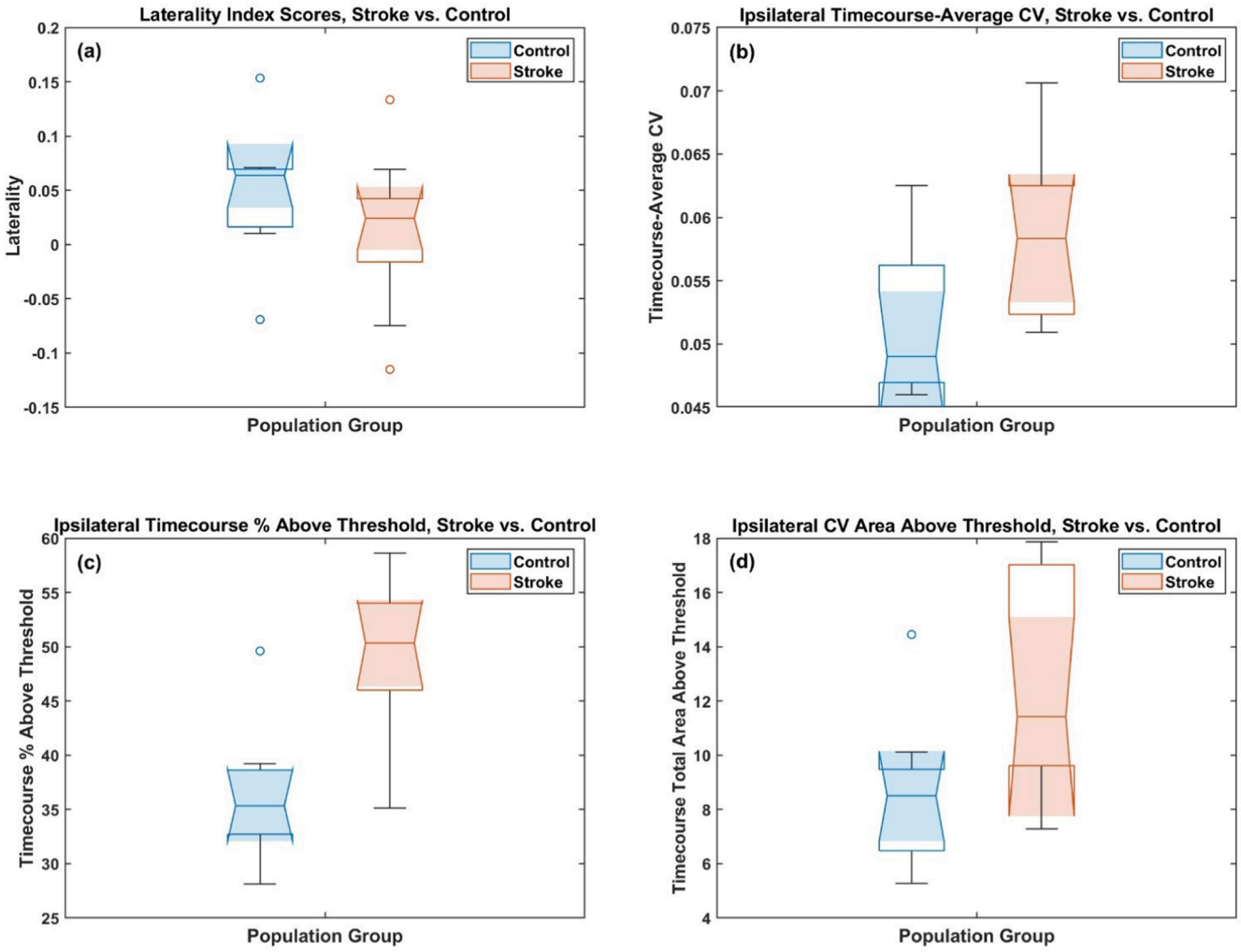

Fig. 5. Control (blue) vs. Stroke (red) population distributions. The median value for each distribution is shown as the central line inside the box plot, with the upper and lower quartiles as box edges, and the range given as the lines above and below the box. Outlier values are shown as circles above and below the range demarcations. Fig. 5a (upper left) shows the laterality index distributions of stroke and control populations. These distributions were not shown to belong to two different populations with 95 % or higher confidence ($p = 0.27$). Fig. 5b (upper right) shows the coherence-time course average value of the EEG/EMG data ipsilateral to the abducted arm (contralesional for stroke participants). The stroke and control average CV distributions represent two statistically different population distributions ($p = 0.032$). Fig. 5c (lower left) shows the percentage of the 1-second EEG-EMG M−PLV time course data (similar to the example in [Fig. 2]) ipsilateral to the abducted arm (contralesional for stroke participants) that was determined to be above the 95 % significance threshold calculated via Monte-Carlo simulation. The stroke and control average CV distributions represent two statistically different population distributions ($p = 0.0017$). Fig. 5d (lower right) shows the total area of the 1-second EEG-EMG M−PLV time course data (similar to the example in [Fig. 2]) ipsilateral to the abducted arm (contralesional for stroke participants) that was determined to be above the 95 % significance threshold calculated via Monte-Carlo simulation. The stroke and control average CV distributions represent two statistically different population distributions ($p = 0.026$).

4. Conclusions and future work

Many individuals with a stroke suffer from upper limb impairment and a lower quality of life for months or years after the initial incident and individuals post-stroke exhibit neural reorganization and increased activity in the motor cortex ipsilateral to the paretic side following recovery. Thus, understanding the mechanisms behind natural post-stroke outcomes and neuroadaptation could lead to a potential optimization of post-stroke rehabilitation interventions, which remains a priority in patient care, especially in moderately to severely impaired individuals with a hemiparetic stroke.

Here, we have explored chronic upper-limb motor recovery outcomes using phase coherence analysis during a shoulder abduction task with 10 S participants and 8 control participants. Multimodal ipsilateral and contralateral data collected via EEG analysis, and deltoid muscle electrical activity collected via EMG electrodes shows a substantial increase in the nerve conduction delay to the deltoid muscle in post-stroke survivors. Furthermore, using M−PLV based phase coherence analysis between EEG and EMG data, we have provided evidence for post-stroke contralesional motor cortex adaptation leading to its increased role in the paretic shoulder abduction task as compared to healthy control participants. When studying the contralesional motor cortex (ipsilateral to the paretic/tested arm) and comparing phase-coherence values, CV time course area above the significance threshold, and percentage time course over this threshold, stroke and healthy control participants exhibited statistically different values. This demonstrates that beta-band contralesional motor cortex behavior is significantly altered in chronic stroke resulting in motor deficits. Beta-band M−PLV phase coherence analysis of the ipsilateral and contralateral motor cortexes in stroke and control participants in this study also shows phase-coherence distribution convergence between the two motor cortexes in stroke participants as compared to control participants. This convergence provides evidence of neural adaptation in the contralesional motor cortex in chronic stroke survivors, due to losses of ipsilesional motor cortical input. While

Table 3
Individual subject results; calculated ipsilateral MPLV values for average coherence values (CV), 95 % significance threshold levels, timecourse percentages above significance threshold (%AT) and MPLV area above significance threshold (AAT).

Participant Number	Control Average Coherence (CV)	Stroke Average Coherence (CV)	Control 95 % Significance Threshold	Stroke 95 % Significance Threshold	Control Timecourse% Above Threshold	Stroke Timecourse% Above Threshold	Control Area Above Threshold	Stroke Area Above Threshold
1	0.0566	0.0706	0.0597	0.0630	39.21	57.52	10.13	17.87
2	0.0469	0.0649	0.0567	0.0560	35.99	58.64	5.70	17.48
3	0.0495	0.0605	0.0574	0.0572	34.72	51.07	5.28	12.13
4	0.0558	0.0545	0.0599	0.0547	38.04	46.04	8.68	10.72
5	0.0625	0.0517	0.0579	0.0533	49.61	46.00	14.45	8.82
6	0.0485	0.0562	0.0561	0.0566	34.33	49.57	8.31	10.39
7	0.0460	0.0509	0.0583	0.0575	31.10	35.11	8.83	9.61
8	0.0470	0.0625	0.0601	0.0557	28.13	54.00	7.26	15.05
9		0.0621		0.0553		51.51		17.02
10		0.0523		0.0586		39.75		7.29
Average	0.0516	0.0586	0.0583	0.0568	36.39	48.92	8.58	12.64

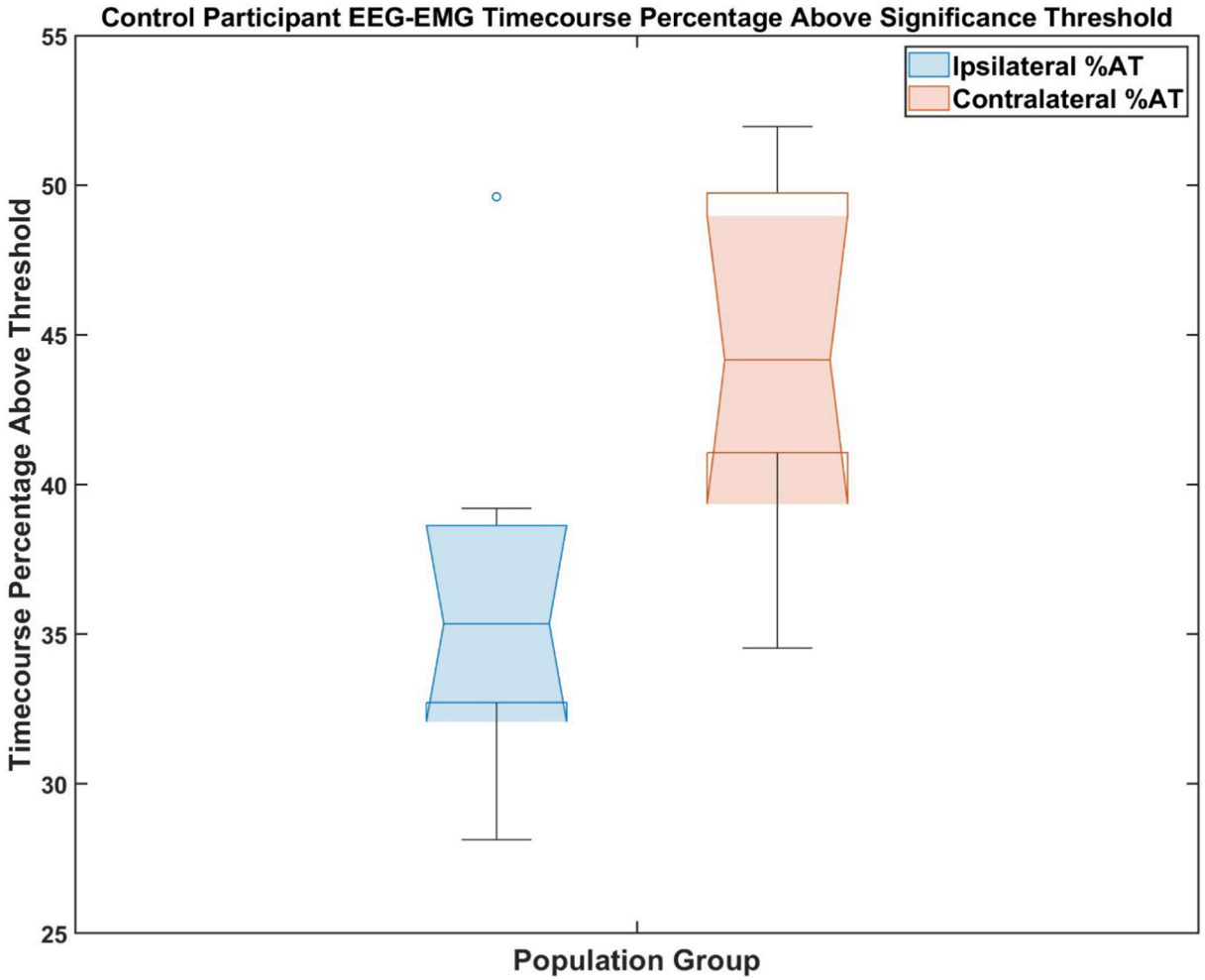

Fig. 6. Percentage of the 1-second EEG-EMG M−PLV CV time course determined to be above the 95 % significance threshold (%AT, calculated via Monte-Carlo simulation) in control participants. The blue population represents the per-subject average CV data from the deltoid EMG electrodes and the central motor cortex EEG electrode ipsilateral to the tested arm, while the red population represents the per-subject average CV data from the deltoid EMG electrodes and the central motor cortex EEG electrode contralateral to the tested arm. The median value for each distribution is shown as the central line inside the box plot, with the upper and lower quartiles as box edges, and the range given as the lines above and below the box. The blue circle above the upper range demarcation for the ipsilateral population represents an outlier value. In control participants, the ipsilateral and contralateral %AT value distributions represent two statistically different population distributions ($p = 0.019$). This data shows that the contralateral motor cortex experiencing significant beta-band EEG-EMG coherence for a longer period of the abduction task than the ipsilateral motor cortex. This is indicative of the differing responsibilities of the two motor cortexes during the normal-function single-arm abduction task.

Table 4
Individual subject results; calculated contralateral MPLV values for average coherence values (CV), 95 % significance threshold levels, timecourse percentages above significance threshold (%AT) and MPLV area above significance threshold (AAT).

Participant Number	Control Average Coherence (CV)	Stroke Average Coherence (CV)	Control 95 % Significance Threshold	Stroke 95 % Significance Threshold	Control Timecourse% Above Threshold	Stroke Timecourse% Above Threshold	Control Area Above Threshold	Stroke Area Above Threshold
1	0.0626	0.0666	0.0580	0.0634	51.37	55.71	15.07	12.08
2	0.0541	0.0594	0.0544	0.0535	48.10	55.32	9.22	15.05
3	0.0539	0.0570	0.0576	0.0568	43.21	44.87	8.93	11.40
4	0.0546	0.0576	0.0575	0.0589	45.11	41.75	8.36	12.04
5	0.0567	0.0587	0.0580	0.0530	39.94	58.01	13.34	14.27
6	0.0486	0.0649	0.0578	0.0556	34.52	50.63	5.80	19.43
7	0.0578	0.0535	0.0581	0.0577	42.19	44.63	12.89	8.17
8	0.0653	0.0605	0.0568	0.0579	51.95	52.44	17.47	12.03
9		0.0515		0.0540		38.62		8.45
10		0.0688		0.0578		62.40		20.20
Average	0.0567	0.0598	0.0573	0.0569	44.55	50.44	11.38	13.31

this convergence likely increases the overall shoulder abduction ability of stroke survivors, previous work has demonstrated that this reorganization simultaneously increases the expression of debilitating flexion synergy as expressed in the coactivation of shoulder, elbow, wrist, and finger muscles, decreasing paretic arm reach, work area, hand opening ability, and fine motor control [52,37,32,38,55].

Expanding this study via the recruitment of additional control participants and stroke participants with varying degrees of upper-limb mobility would further confirm these phase-coherence results. A larger study involving a larger population of stroke participants could also enable further sub-classification of contralesional motor cortex adaptation and nerve conduction delay by stroke severity. Such a study may be effective in linking motor impairment level to other parameters discussed in this study, such as response delay latency and EEG-EMG coherence values, as our data shows no significant correlation between clinical assessment scores (e.g., Fugl-Meyer Upper Extremity Assessment) or more quantitative measures of synergies and spasticity [51]and coherence values for the limited number of stroke participants we studied. This larger study would focus on the role of increased post-stroke contralesional motor cortex recruitment in the loss of paretic arm functionality resulting from the increased reliance on cortico-reticulospinal pathways, causing the expression of the flexion synergy, not only in chronic, but also its development from acute and subacute hemiparetic stroke. Additionally, while our pilot study measured chronic upper-limb related beta-band cortico-muscular phase coherence, if stroke participants were to be tested multiple times, starting immediately after their stroke into the chronic phase (>6 months post-stroke), such a study would allow for the characterization of coherence changes during the post-stroke recovery process.

Funding

This work was supported by NIH/NICHD R21HD099710 (PIs: Dewald and Yang) and NIH/NICHD R01 HD109157 (PI: Yang), Dr. Yang's time on this work was also supported by his American Heart Association Award (932980) and National Science Foundation (NSF 2401215). Dr. Dewald's time on this research was also supported by his NIH/NINDS R01NS105759.

CRediT authorship contribution statement

Nishaal Parmar: Writing – original draft, Methodology, Investigation. **Parikshat Sirpal:** Writing – review & editing. **William A Sikora:** Writing – review & editing. **Julius P.A. Dewald:** Writing – review & editing, Funding acquisition. **Hazem H. Refai:** Writing – review & editing. **Yuan Yang:** Writing – review & editing, Supervision, Project administration, Funding acquisition, Conceptualization.

Declaration of competing interest

The authors declare that they have no known competing financial interests or personal relationships that could have appeared to influence the work reported in this paper.

Data availability

Data will be made available on request.

Acknowledgments

The authors want to thank Mr. Runfeng Tian for his assistance in data collection.

Ethics Statement

All data collected in this study was approved by the Institutional Review Board (IRB) at Northwestern University (STU0021840), USA, and participants provided informed consent prior to study participation.

References

[1] S. Anwer, A. Waris, S.O. Gilani, J. Iqbal, N. Shaikh, A.N. Pujari, I.K. Niazi, January. Rehabilitation of upper limb motor impairment in stroke: A narrative review on the prevalence, risk factors, and economic statistics of stroke and state of the art therapies, Healthcare 10 (2) (2022) 190.
[2] K.B. Baker, et al., Cerebellar deep brain stimulation for chronic post-stroke motor rehabilitation: a phase I trial, Nat. Med. 29 (9) (2023) 2366–2374.
[3] Z. Bayraktaroglu, K. von Carlowitz-Ghori, G. Curio, V.V. Nikulin, It is not all about phase: amplitude dynamics in corticomuscular interactions, Neuroimage 64 (2013) 496–504.
[4] B. Boashash, Estimating and interpreting the instantaneous frequency of a signal. I. Fundamentals, Proc. IEEE 80 (4) (1992) 520–538.
[5] M.R. Borich, C. Mang, L.A. Boyd, Both projection and commissural pathways are disrupted in individuals with chronic stroke: investigating microstructural white matter correlates of motor recovery, BMC Neurosci. 13 (1) (2012) 1–11.
[6] Brunnstrom, S., 1970. Movement therapy in hemiplegia. A neurophysiological approach. New York: Harper & Row.
[7] S.F. Campfens, H. van der Kooij, A.C. Schouten, Face to phase: pitfalls in time delay estimation from coherency phase, J. Comput. Neurosci. 37 (2014) 1–8.
[8] W.-T. Chien, et al., Robot-assisted therapy for upper-limb rehabilitation in subacute stroke patients: A systematic review and meta-analysis, Brain and Behavior 10 (8) (2020) e01742.
[9] A. Chowdhury, A. Dutta, G. Prasad, Corticomuscular co-activation based hybrid brain-computer interface for motor recovery monitoring, IEEE Access 8 (2020) 174542–174557.
[10] da Silva Costa, Andréia Abud, et al. (2024)"Corticomuscular and intermuscular coherence as a function of age and walking balance difficulty." Neurobiology of Aging, 141:85-101.
[11] A. Delorme, S. Makeig, EEGLAB: an open-source toolbox for analysis of single-trial EEG dynamics, J. Neurosci. Methods 134 (2004) 9–21.
[12] Dewald, J.P., Ellis, M.D., Acosta, A.M., Sohn, M.H. and Plaisier, T.A., 2022. Implementation of impairment-based neurorehabilitation devices and technologies

following brain injury. In Neurorehabilitation technology (pp. 89-112). Cham: Springer International Publishing.
[13] M.D. Ellis, C. Carmona, J. Drogos, J.P. Dewald, Progressive abduction loading therapy with horizontal-plane viscous resistance targeting weakness and flexion synergy to treat upper limb function in chronic hemiparetic stroke: a randomized clinical trial, Front. Neurol. 9 (2018) 71.
[14] M.D. Ellis, I. Schut, J.P. Dewald, Flexion synergy overshadows flexor spasticity during reaching in chronic moderate to severe hemiparetic stroke, Clin. Neurophysiol. 128 (7) (2017) 1308–1314.
[15] M.D. Ellis, T.M. Sukal-Moulton, J.P. Dewald, Impairment-based 3-D robotic intervention improves upper extremity work area in chronic stroke: targeting abnormal joint torque coupling with progressive shoulder abduction loading, IEEE Trans. Rob. 25 (3) (2009) 549–555.
[16] M.D. Ellis, T. Sukal-Moulton, J.P. Dewald, Progressive shoulder abduction loading is a crucial element of arm rehabilitation in chronic stroke, Neurorehabil. Neural Repair 23 (8) (2009) 862–869.
[17] G.B. Ermentrout, n: m Phase-locking of weakly coupled oscillators, J. Math. Biol. 12 (3) (1981) 327–342.
[18] J.N. Williamson, W.A. Sikora, S.A. James, N.J. Parmar, L.V. Lepak, C.F. Cheema, H. H. Refai, D.H. Wu, E.V. Sidorov, J.P. Dewald, Y. Yang, Cortical reorganization of early somatosensory processing in hemiparetic stroke, J. Clin. Med. 11 (21) (2022) 6449.
[19] M. Fabri, G. Polonara, M.D. Pesce, A. Quattrini, U. Salvolini, T. Manzoni, Posterior corpus callosum and interhemispheric transfer of somatosensory information: an fMRI and neuropsychological study of a partially callosotomized patient, J. Cogn. Neurosci. 13 (8) (2001) 1071–1079.
[20] D. Farina, F. Negro, N. Jiang, Identification of common synaptic inputs to motor neurons from the rectified electromyogram, J. Physiol. 591 (10) (2013) 2403–2418.
[21] Fiore, Stefano, et al. "The effectiveness of robotic rehabilitation for the functional recovery of the upper limb in post-stroke patients: A systematic review." Retos: nuevas tendencias en educación física, deporte y recreación 50 (2023): 91-101.
[22] M. Franceschini, F. La Porta, M. Agosti, M. Massucci, Is health-related quality of life of stroke patients influenced by neurological impairments at one year after stroke? Eur. J. Phys. Rehabil. Med. 46 (2010) 389–399.
[23] Z. Gao, et al., Influencing factors of corticomuscular coherence in stroke patients, Front. Hum. Neurosci. 18 (2024) 1354332.
[24] C. Grefkes, G.R. Fink, Reorganization of cerebral networks after stroke: new insights from neuroimaging with connectivity approaches, Brain 134 (5) (2011) 1264–1276.
[25] C.D. Guerrero-Mendez, A.F. Ruiz-Olaya, Coherence-based connectivity analysis of EEG and EMG signals during reach-to-grasp movement involving two weights, Brain-Computer Interf. 9 (3) (2022) 140–154.
[26] Z. Guo, Q. Qian, K. Wong, H. Zhu, Y. Huang, X. Hu, Y. Zheng, Altered corticomuscular coherence (CMCoh) pattern in the upper limb during finger movements after stroke, Front. Neurol. 11 (2020) 521202.
[27] Y. Yang, T. Solis-Escalante, J. Yao, A. Daffertshofer, A.C. Schouten, F.C. Van Der Helm, A general approach for quantifying nonlinear connectivity in the nervous system based on phase coupling, Int. J. Neural Syst. 26 (01) (2016) 1550031.
[28] C. Höhler, et al., The efficacy of hybrid neuroprostheses in the rehabilitation of upper limb impairment after stroke, a narrative and systematic review with a meta-analysis, Artif. Organs 48 (3) (2024) 232–253.
[29] H. Karbasforoushan, J. Cohen-Adad, J. Dewald, Brainstem and spinal cord MRI identifies altered sensorimotor pathways post-stroke, Nat. Commun. 10 (1) (2019) 1–7.
[30] F. Khademi, et al., Rewiring cortico-muscular control in the healthy and poststroke human brain with proprioceptive β-Band neurofeedback, J. Neurosci. 42 (36) (2022) 6861–6877.
[31] P. Langhorne, J. Bernhardt, G. Kwakkel, Stroke rehabilitation, Lancet 377 (9778) (2011) 1693–1702.
[32] Y. Lan, J. Yao, J.P. Dewald, The impact of shoulder abduction loading on volitional hand opening and grasping in chronic hemiparetic stroke, Neurorehabil. Neural Repair 31 (6) (2017) 521–529.
[33] S. Li, Y.T. Chen, G.E. Francisco, P. Zhou, W.Z. Rymer, A unifying pathophysiological account for post-stroke spasticity and disordered motor control, Front. Neurol. 10 (2019) 446064.
[34] Li, S., G. E. Francisco and W. Z. Rymer (2021). "A New Definition of Poststroke Spasticity and and the Interference of Spasticity With Motor Recovery From Acute to Chronic Stages." Neurorehabilitation and Neural Repair: 35(7), 601-610.
[35] Williamson, Jordan N., Shirley A. James, Dorothy He, Sheng Li, Evgeny V. Sidorov, and Yuan Yang. "High-definition transcranial direct current stimulation for upper extremity rehabilitation in moderate-to-severe ischemic stroke: a pilot study." ***Front. hum. neurosci.*** 17 (2023): 1286238.
[36] A.C. Lo, P.D. Guarino, L.G. Richards, J.K. Haselkorn, G.F. Wittenberg, et al., Robot-assisted therapy for long-term upperlimb impairment after stroke, N. Engl. J. Med. 362 (19) (2010) 1772–1783.
[37] J.G. McPherson, A. Chen, M.D. Ellis, J. Yao, C.J. Heckman, J.P. Dewald, Progressive recruitment of contralesional cortico-reticulospinal pathways drives motor impairment post stroke, J. Physiol. 596 (7) (2018) 1211–1225.
[38] L.M. McPherson, J.P. Dewald, Abnormal synergies and associated reactions post-hemiparetic stroke reflect muscle activation patterns of brainstem motor pathways, Front. Neurol. 13 (2022).
[39] J.R. Millán, R. Rupp, G. Mueller-Putz, R. Murray-Smith, C. Giugliemma, M. Tangermann, C. Vidaurre, F. Cincotti, A. Kubler, R. Leeb, Combining brain–computer interfaces and assistive technologies: state-of-the-art and challenges, in: Front. Neurosci., 4, 2010, p. 161.
[40] Mima, Tatsuya, Takahiro Matsuoka, and Mark Hallett. "Information flow from the sensorimotor cortex to muscle in humans." Clinical Neurophysiology 112.1 (2001): 122-126.Mozaffarian, Dariush, et al. "Heart disease and stroke statistics—2015 update: a report from the American Heart Association." circulation 131.4 (2015): e29-e322.
[41] S.D. Muthukumaraswamy, B.W. Johnson, Primary motor cortex activation during action observation revealed by wavelet analysis of the EEG, Clin. Neurophysiol. 115 (8) (2004) 1760–1766.
[42] L.J. Myers, et al., Rectification and non-linear pre-processing of EMG signals for cortico-muscular analysis, J. Neurosci. Methods 124 (2) (2003) 157–165.
[43] National Institute of Neurological Disorders, Stroke (US). Office of Communications and Public Liaison, 1999. Stroke: Hope through research (No. 99). The Institute.
[44] M. Owen, C. Ingo, J. Dewald, Upper extremity motor impairments and microstructural changes in bulbospinal pathways in chronic hemiparetic stroke, Front. Neurol. 8 (2017) 257.
[45] E. Pardo-Igúzquiza, F.J. Rodríguez-Tovar, Spectral and cross-spectral analysis of uneven time series with the smoothed Lomb-Scargle periodogram and Monte Carlo evaluation of statistical significance, Comput. Geosci. 49 (2012) 207–216.
[46] M.J.L. Perenboom, M. Van de Ruit, J.H. De Groot, A.C. Schouten, C.G.M. Meskers, Evidence for sustained cortical involvement in peripheral stretch reflex during the full long latency reflex period, Neurosci. Lett. 584 (2015) 214–218.
[47] F. Pichiorri, et al., Exploring high-density corticomuscular networks after stroke to enable a hybrid Brain-Computer Interface for hand motor rehabilitation, J. Neuroeng. Rehabil. 20 (1) (2023) 5.
[48] Pollock A, Farmer SE, Brady MC, Langhorne P, Mead GE, Mehrholz J, van Wijck F. Interventions for improving upper limb function after stroke. The Cochrane database of systematic reviews. 2013;11.
[49] H. Rodgers, et al., Robot assisted training for the upper limb after stroke (RATULS): a multicentre randomised controlled trial, Lancet 394 (10192) (2019) 51–62.
[50] P. Sirpal, R. Damseh, K. Peng, D.K. Nguyen, F. Lesage, Multimodal autoencoder predicts fNIRS resting state from EEG signals, Neuroinformatics 20 (3) (2022) 537–558.
[51] Sinha N, Dewald JPA, Yang, Y. (2024), Perturbation-induced electromyographic activity is predictive of flexion synergy expression and a sensitive measure of post-stroke motor impairment. the 46th Annual International Conference of the IEEE Engineering in Medicine and Biology Society (IEEE EMBC 2024), Orlando, Florida, July 15-19, 2024.
[52] T.M. Sukal, M.D. Ellis, J.P. Dewald, Shoulder abduction-induced reductions in reaching work area following hemiparetic stroke: neuroscientific implications, Exp. Brain Res. 183 (2007) 215–223.
[53] U. Sveen, E. Bautz-Holter, K.M. Sodring, T.G. Wyller, K. Laake, Association between impairments, self-care ability and social activities 1 year after stroke, Disabil. Rehabil. 21 (8) (1999) 372–377.
[54] A.G. Thompson-Butel, et al., Additional therapy promotes a continued pattern of improvement in upper-limb function and independence post-stroke, J. Stroke Cerebrovasc. Dis. 32 (4) (2023) 106995.
[55] R. Tian, J.P. Dewald, Y. Yang, Assessing the usage of indirect motor pathways following a hemiparetic stroke, IEEE Trans. Neural Syst. Rehabil. Eng. 29 (2021) 1568–1572.
[56] K. Von Carlowitz-Ghori, Z. Bayraktaroglu, F.U. Hohlefeld, F. Losch, G. Curio, V. V. Nikulin, Corticomuscular coherence in acute and chronic stroke, Clin. Neurophysiol. 125 (6) (2014) 1182–1191.
[57] Van Der Helm N. A., N. Gurari, J. M. Drogos and J. P. Dewald. Task directionality impacts the ability of individuals with chronic hemiparetic stroke to match torques between arms: Preliminary findings. In: Rehabilitation Robotics (ICORR), 2017 International Conference on IEEE, 2017, p. 714–719.
[58] V. der Vliet Rick, et al., Predicting upper limb motor impairment recovery after stroke: a mixture model, Ann. Neurol. 87 (3) (2020) 383–393.
[59] B. Vasudeva, R. Tian, D.H. Wu, S.A. James, H.H. Refai, L. Ding, F. He, Y. Yang, Multi-phase locking value: A generalized method for determining instantaneous multi-frequency phase coupling, Biomed. Signal Process. Control 74 (2022) 103492.
[60] J.M. Veerbeek, A.C. Langbroek-Amersfoort, E.E. Van Wegen, C.G. Meskers, G. Kwakkel, Effects of robot-assisted therapy for the upper limb after stroke: a systematic review and meta-analysis, Neurorehabil. Neural Repair 31 (2) (2017) 107–121.
[61] S.S. Virani, A. Alonso, H.J. Aparicio, E.J. Benjamin, M.S. Bittencourt, C. W. Callaway, et al., Heart disease and stroke statistics—2021 update: a report from the American Heart Association, Circulation 143 (8) (2021) e254–e743, https://doi.org/10.1161/CIR.0000000000000950.
[62] G. Wang, et al., Multisensory conflict impairs cortico-muscular network connectivity and postural stability: insights from partial directed coherence analysis, Neurosci. Bull. 40 (1) (2024) 79–89.
[63] S. Wang, M. Tang, Exact confidence interval for magnitude-squared coherence estimates, IEEE Signal Process Lett. 11 (3) (2004) 326–329.
[64] T. Wang, et al., Evaluating stroke rehabilitation using brain functional network and corticomuscular coupling, Int. J. Neurosci. 134 (3) (2024) 234–242.
[65] K.B. Wilkins, M. Owen, C. Ingo, C. Carmona, J.P. Dewald, J. Yao, Neural plasticity in moderate to severe chronic stroke following a device-assisted task-specific arm/hand intervention, Front. Neurol. 8 (2017) 284.
[66] E.R. Williams, S.N. Baker, Renshaw cell recurrent inhibition improves physiological tremor by reducing corticomuscular coupling at 10 Hz, J. Neurosci. 29 (20) (2009) 6616–6624.

[67] C.L. Witham, M. Wang, S.N. Baker, Corticomuscular coherence between motor cortex, somatosensory areas and forearm muscles in the monkey, Front. Syst. Neurosci. 4 (2010) 38.
[68] C.L. Witham, C.N. Riddle, M.R. Baker, S.N. Baker, Contributions of descending and ascending pathways to corticomuscular coherence in humans, J. Physiol. 589 (15) (2011) 3789–3800.
[69] T. Wyller, U. Sveen, K. Sodring, A. Pettersen, E. Bautz-Holter, Subjective well-being one year after stroke, Clin. Rehabil. 11 (1997) 139–145.
[70] R. Xu, et al., Lower-limb motor assessment with corticomuscular coherence of multiple muscles during ankle dorsiflexion after stroke, IEEE Trans. Neural Syst. Rehabil. Eng. 31 (2022) 160–168.
[71] E. Yamanaka, Y. Horiuchi, I. Nojima, EMG-EMG coherence during voluntary control of human standing tasks: a systematic scoping review, Front. Neurosci. 17 (2023) 1145751.
[72] Y. Yang, N. Sinha, R. Tian, N. Gurari, J.M. Drogos, J.P.A. Dewald, Quantifying altered neural connectivity of the stretch reflex in chronic hemiparetic stroke, IEEE Trans. Neural Syst. Rehabil. Eng. 28 (6) (2020) 1436–1441.
[73] Y. Yang, et al., Nonlinear coupling between cortical oscillations and muscle activity during isotonic wrist flexion, Front. Comput. Neurosci. 10 (2016) 126.
[74] Y. Yang, J.P. Dewald, F.C. van der Helm, A.C. Schouten, Unveiling neural coupling within the sensorimotor system: directionality and nonlinearity, Eur. J. Neurosci. 48 (7) (2018) 2407–2415.
[75] Hernández Niño, Juan David, et al. "Functional electrostimulation for upper limbs after stroke: a systematic review." (2022): 1073-1083.
[76] X. Zhang, et al., The corticomuscular coupling underlying movement and its application for rehabilitation: A review, Brain-Apparatus Commun.: A J. Bacomics 2 (1) (2023) 2183096.
[77] Lu. Zhou, et al., Cortico-muscular coherence of time–frequency and spatial characteristics under movement observation, movement execution, and movement imagery, Cogn. Neurodyn. (2023) 1–18.
[78] S. Zhou, et al., Pathway-specific cortico-muscular coherence in proximal-to-distal compensation during fine motor control of finger extension after stroke, J. Neural Eng. 18 (5) (2021) 056034.